

# SIK3 is essential for chondrocyte hypertrophy during skeletal development in mice

Satoru Sasagawa<sup>1,3,6</sup>, Hiroshi Takemori<sup>4</sup>, Tatsuya Uebi<sup>4</sup>, Daisuke Ikegami<sup>1,2</sup>, Kunihiro Hiramatsu<sup>1,2</sup>, Shiro Ikegawa<sup>5</sup>, Hideki Yoshikawa<sup>2</sup> and Noriyuki Tsumaki<sup>1,2,3,7,\*</sup>

## SUMMARY

Chondrocyte hypertrophy is crucial for endochondral ossification, but the mechanism underlying this process is not fully understood. We report that salt-inducible kinase 3 (SIK3) deficiency causes severe inhibition of chondrocyte hypertrophy in mice. SIK3-deficient mice showed dwarfism as they aged, whereas body size was unaffected during embryogenesis. Anatomical and histological analyses revealed marked expansion of the growth plate and articular cartilage regions in the limbs, accumulation of chondrocytes in the sternum, ribs and spine, and impaired skull bone formation in SIK3-deficient mice. The primary phenotype in the skeletal tissue of SIK3-deficient mice was in the humerus at E14.5, where chondrocyte hypertrophy was markedly delayed. Chondrocyte hypertrophy was severely blocked until E18.5, and the proliferative chondrocytes occupied the inside of the humerus. Consistent with impaired chondrocyte hypertrophy in SIK3-deficient mice, native SIK3 expression was detected in the cytoplasm of prehypertrophic and hypertrophic chondrocytes in developing bones in embryos and in the growth plates in postnatal mice. HDAC4, a crucial repressor of chondrocyte hypertrophy, remained in the nuclei in SIK3-deficient chondrocytes, but was localized in the cytoplasm in wild-type hypertrophic chondrocytes. Molecular and cellular analyses demonstrated that SIK3 was required for anchoring HDAC4 in the cytoplasm, thereby releasing MEF2C, a crucial facilitator of chondrocyte hypertrophy, from suppression by HDAC4 in nuclei. Chondrocyte-specific overexpression of SIK3 induced closure of growth plates in adulthood, and the SIK3-deficient cartilage phenotype was rescued by transgenic SIK3 expression in the humerus. These results demonstrate an essential role for SIK3 in facilitating chondrocyte hypertrophy during skeletogenesis and growth plate maintenance.

**KEY WORDS:** *Col11a2*, HDAC4, SIK3, Chondrocyte hypertrophy, Endochondral bone formation, Knockout mouse

## INTRODUCTION

Vertebrate bones develop through membranous or endochondral ossification. Except for craniofacial bones and the clavicle, all bones are established through the latter process (Olsen et al., 2000; Karsenty et al., 2009). At the onset of endochondral bone formation, mesenchymal cells first undergo condensation, followed by differentiation of cells within these condensations into chondrocytes. Chondrocytes then proliferate and produce extracellular matrix to form the primordial cartilage that prefigures the future skeletal elements. Shortly after the formation of the primordial cartilage, proliferating chondrocytes in the central region of the cartilage exit the cell cycle and differentiate into prehypertrophic, and subsequently hypertrophic, chondrocytes. The proliferating chondrocytes closest to the prehypertrophic chondrocytes flatten out and form orderly columns of flat chondrocytes that continue to proliferate. Finally, hypertrophic chondrocytes progress to terminal maturation, following which they express matrix metalloproteinase

13 (MMP13). The terminally matured chondrocytes undergo apoptosis. Blood vessels, along with osteoblasts, osteoclasts and hematopoietic cells, then invade this region and form primary ossification centers. Within these centers, the hypertrophic cartilage matrix is degraded, the hypertrophic chondrocytes die, and bone replaces the disappearing cartilage.

Recent molecular and genetic studies coupled with classical histological approaches have revealed many of the factors that are involved in endochondral bone formation (Lefebvre and Smits, 2005). For example, SOX9 is expressed in mesenchymal progenitor cells and in chondrocytes, but its expression ceases in prehypertrophic chondrocytes (Ng et al., 1997; Zhao et al., 1997). SOX9 has a variety of functions in chondrogenesis: its expression in mesenchymal progenitor cells is essential for cartilage formation (Akiyama et al., 2002); it directly regulates cartilage-specific matrix genes such as the  $\alpha 1$ (II) collagen chain gene (*Col2a1*), aggrecan (*Acan*) and the  $\alpha 2$ (XI) collagen chain gene (*Col11a2*); it sustains the survival of proliferative chondrocytes during development (Ikegami et al., 2011); SOX9 overexpression in proliferative chondrocytes suppresses their hypertrophy (Akiyama et al., 2004); and it negatively regulates the transcription of the gene that encodes vascular endothelial growth factor (VEGF), which is expressed by hypertrophic chondrocytes (Hattori et al., 2010).

Regarding the hypertrophic differentiation of chondrocytes, several crucial transcriptional regulators have been identified. Histone deacetylase 4 (HDAC4), a class II HDAC, represses the expression of multiple genes through chromatin remodeling, thereby regulating cell fate. To elucidate the specific role of HDAC4, *Hdac4*-null mice have been generated and were noted to display dwarfism and inappropriate chondrocyte hypertrophy,

<sup>1</sup>Department of Bone and Cartilage Biology, Graduate School of Medicine, Osaka University, 2-2 Yamadaoka, Suita, Osaka 565-0871, Japan. <sup>2</sup>Department of Orthopedic Surgery, Graduate School of Medicine, Osaka University, 2-2 Yamadaoka, Suita, Osaka 565-0871, Japan. <sup>3</sup>Japan Science and Technology Agency, CREST, Tokyo, 102-0075, Japan. <sup>4</sup>Laboratory of Cell Signal and Metabolism, National Institute of Biomedical Innovation, 7-6-9 Asagi, Ibaraki, Osaka 567-0085, Japan. <sup>5</sup>Laboratory of Bone and Joint Diseases, Center for Genomic Medicine, RIKEN, Tokyo 108-8639, Japan. <sup>6</sup>Department of Biology, Osaka Medical Center for Cancer and Cardiovascular Diseases, Osaka 537-0025, Japan. <sup>7</sup>Center for iPS Cell Research and Application, Kyoto-University, 53 Kawahara-cho, Shogoin, Sakyo-ku, Kyoto 606-8507, Japan.

\* Author for correspondence (ntsumaki@cira.kyoto-u.ac.jp)

leading to ectopic bone formation. By contrast, the overexpression of HDAC4 in proliferative chondrocytes inhibited chondrocyte hypertrophy (Vega et al., 2004).

The transcription factor RUNX2 (CBFA1) is a key regulator of osteoblast differentiation. When RUNX2-deficient mice were generated, a lack of chondrocyte hypertrophy was found, suggesting that RUNX2 might regulate chondrocyte hypertrophy as does HDAC4 (Komori et al., 1997). To address this possibility, non-hypertrophic chondrocyte-specific *Runx2* transgenic mice were generated. These animals showed ectopic chondrocyte hypertrophy and enhanced endochondral ossification (Takeda et al., 2001). MEF2C is a crucial transcription factor in muscle and cardiovascular development. To clarify its role in chondrogenesis, cartilage-specific conditional *Mef2c* deletion mice and cartilage-specific dominant-negative and dominant-active MEF2C mice were generated, and these demonstrated a positive role for MEF2C in chondrocyte hypertrophy (Arnold et al., 2007). Genetically, the mild phenotype in the sternum of *Mef2c*<sup>+/-</sup> pups was rescued by deletion of one copy of the *Hdac4* gene, demonstrating that it depends on a balance between transcriptional activation by MEF2C and repression by HDAC4 (Arnold et al., 2007). In addition, HDAC4 interacts directly with RUNX2 to repress its transcriptional activity on the type X collagen promoter (Vega et al., 2004). Therefore, HDAC4 is thought to be a central negative regulator of chondrocyte hypertrophy.

With regard to the regulation of HDAC4 activity in chondrocyte hypertrophy, a recent study proposed that phosphatase PP2A, which is activated by the PTHrP-cAMP-PKA cascade in chondrocytes, dephosphorylates HDAC4 to turn on its activity and to potentiate its localization in nuclei, thereby inhibiting chondrocyte hypertrophy (Kozhemyakina et al., 2009). However, the regulatory mechanisms that suppress the transcriptional repression activity of HDAC4 in chondrocytes have not been reported so far.

Salt-inducible kinase 3 (SIK3, also known as QSK) is a member of the 5'-AMP-activated protein kinase (AMPK) family. SIK3 belongs to the SIK subfamily, which also includes SIK1 (also known as MSK or SNF1LK) and SIK2 (also known as QIK) (Katoh et al., 2004). Mammalian SIK1 and SIK2 are currently being characterized in terms of their function in various biological processes and molecular regulatory mechanisms. Recently, fly SIK3 (the homolog of mouse SIK2) was shown to sequester HDAC4 in the cytoplasm and to regulate the energy balance in the *Drosophila* fat body (Wang et al., 2011). Compared with SIK1 and SIK2, the function of SIK3 is poorly understood. To understand SIK3 function in vertebrates, we generated SIK3-deficient mice. The SIK3-deficient mice showed various phenotypes, including bone abnormalities (this study) and impaired cholesterol metabolism (T.U., Y. Itoh, O. Hatano, A. Kumagai, M. Sanosaka, T. Sasaki, S.S., J. Doi, K. Tatsumi, K. Mitamura et al., unpublished). Here, we report a role for SIK3 in skeletal development. By performing anatomical and histological analyses, we clarified that the bone abnormalities in SIK3-deficient mice are due to impaired chondrocyte hypertrophy. We also demonstrated that SIK3 binds directly to HDAC4 and has the capacity to anchor HDAC4 in the cytoplasm. Together, our results establish SIK3 as an essential factor for chondrocyte hypertrophy.

## MATERIALS AND METHODS

### Generation of *Sik3* knockout mice and embryos

The *Sik3* knockout strategy and targeting vector design are shown in supplementary material Fig. S1. Briefly, the PGK-neo cassette was inserted in place of exon 1 of *Sik3*. The successful targeting of embryonic stem cells

was confirmed by Southern blot analysis, and the cells were injected into C57BL/6N blastocysts. To obtain SIK3-deficient embryos, *Sik3* heterozygous male and female mice were mated and wild-type littermates were used as controls.

### Generation of *Col11a2-hSIK3* transgenic mice

The  $\alpha 2(XI)$  collagen gene-based expression vector 742LacZInt contains the mouse *Col11a2* promoter (−742 to +380), an SV40 RNA splice site, the *lacZ* reporter gene, SV40 polyadenylation signal and a 2.3 kb segment of the first intron of *Col11a2* as an enhancer (Tsumaki et al., 1996). To create the human *SIK3* (*hSIK3*) transgene, the *hSIK3* fragment was cloned into the expression vector, replacing the *lacZ* gene, to create *Col11a2-hSIK3*. Transgenic mice were produced by microinjection of the linearized insert into the pronuclei of fertilized eggs from F1 hybrid mice (C57BL/6 × DBA), as described previously (Hiramatsu et al., 2011). Transgenic mice were identified by PCR assays on genomic DNA extracted from the tail. The mice were backcrossed at least eight times to the C57BL/6N strain.

All experiments were approved by the Institutional Animal Care and Use Committee (IACUC) of Osaka University Graduate School of Medicine and the Osaka University Living Modified Organism (LMO) Experiments Safety Committee.

### Cartilage and bone staining

For whole-mount skeletal analysis, mice or embryos were skinned, the internal organs and as much connective tissue as possible, including muscles and tendons, were removed, and the specimens fixed overnight in pure ethanol. The specimens were stained with Alcian Blue and Alizarin Red for 48 hours for embryos or 72 hours for adult mice. After staining, embryos were incubated in 20% glycerol in a 1% KOH solution and adult specimens were incubated in 3% KOH solution at 37°C for 1 day to remove soft tissue. To improve transparency, specimens were cleared in 50% glycerol in a 0.5% KOH solution at 37°C for 2 days, which was then replaced with 80% glycerol solution for completion of the reaction.

### Sectioning and staining

For juvenile and adult mouse samples, specimens were fixed in 10% phosphate-buffered formalin at 4°C for 16–24 hours, followed by decalcification with saturated EDTA solution for 4 days. For embryonic samples, specimens were fixed in 4% PFA in PBS at 4°C for 16 hours, followed by decalcification with saturated EDTA solution for 1 day, except for specimens younger than E18.5 and samples used for von Kossa staining. The samples were embedded in paraffin, sectioned at 3  $\mu$ m, and then subjected to Safranin O and Fast Green staining or von Kossa staining according to standard protocols.

### Immunofluorescent and immunohistochemical staining

Antibodies used for the immunofluorescent analysis of section samples were as follows: mouse anti-type I collagen (Abcam, 1:500), mouse anti-type II collagen (Thermo Scientific, 1:500), mouse anti-type X collagen (Quartett, 1:100), goat anti-MMP13 (Millipore, 1:100), rabbit anti-SOX9 (Santa Cruz Biotechnology, 1:100), mouse anti-PCNA (Santa Cruz, 1:100), rabbit anti-SIK3 (Abcam, 1:100), rabbit anti-HDAC4 (Abcam, 1:100), rabbit anti-MEF2C (Abcam, 1:100), Alexa Fluor-conjugated secondary antibodies (Invitrogen, 1:500) and an HRP-labeled secondary antibody (GE Healthcare, 1:500).

Deparaffinized specimens were incubated in 20 mM Tris-HCl (pH 9.0) at 70°C for 6 hours to retrieve the antigen. For detection of type II collagen, samples were treated with 20  $\mu$ M proteinase K for 10 minutes at 37°C. After blocking with 2% blocking reagent (Roche), the specimens were stained with primary antibody at 4°C overnight, then rinsed twice with PBS, and stained with a secondary antibody for 2 hours, followed by nuclear counterstaining with Hoechst 33342 (Invitrogen, 1:1000) for 30 minutes or, for samples used for detection of type II collagen, with Hematoxylin at room temperature. Specimens were observed using a fluorescence microscope system (Eclipse Ti, Nikon) equipped with a CCD camera (Hamamatsu Photonics). HRP labeling was visualized with DAB reagent (DAKO).



### Cell culture, transfection, pulldown assay and imaging

293FT cells were grown in DMEM containing 10% FBS. ATDC5 cells were grown in DMEM/F-12 medium containing 5% FBS. The *Hdac4* and *Mef2c* cDNAs were cloned from a primary chondrocyte cDNA pool into the pENTR vector (Invitrogen) and their sequences confirmed. The primer sequences used for cloning are listed in supplementary material Table S1. Full-length *Sik3* cDNA was purchased from Invitrogen. For HA-tagged HDAC4 expression, *Hdac4* cDNA was subcloned into the pCMV-HA expression vector (Clontech). To construct an EGFP-HDAC4 fusion expression vector, the *Egfp* gene was subcloned into the 5' region of the *Hdac4* gene in pENTR-HDAC4. For other expression constructs, the cDNAs were transferred into the CMV-driven expression vector using the Gateway system (Invitrogen). For transient transfection, Lipofectamine 2000 (Invitrogen) was used according to the manufacturer's instructions.

The pulldown assay was performed as described previously (Takeda et al., 2006). Briefly, transiently transfected cells were solubilized in RIPA buffer containing protease inhibitor and phosphatase inhibitor (both Roche) 48 hours after transfection. The cell lysates in RIPA buffer were subjected to pulldown assay with the 12CA5 anti-HA or 9E10 anti-Myc antibody (Santa Cruz) and Protein G Sepharose beads (GE Healthcare), were separated on a NuPAGE gel (Invitrogen) and evaluated by a western blotting analysis with the ECL system (PerkinElmer). A ChemiDoc XRS Plus system (BioRad) was used for image development.

For cellular immunofluorescence imaging, cells were fixed in 10% PFA for 30 minutes at room temperature, washed twice with PBS, and then permeabilized with 0.2BT solution (0.2% Triton X-100 and 2 mg/ml BSA in water) for 10 minutes. The specimens were stained with anti-SIK3 antibody (1:500) for 2 hours, followed by an Alexa Fluor-conjugated secondary antibody (1:2000) for 1 hour, and were then counterstained with Hoechst 33342 (1:1000) for 30 minutes at room temperature. The cells were imaged using a fluorescence microscope (Eclipse Ti) equipped with a CCD camera (Hamamatsu Photonics).

MEF2C luciferase reporter assays were performed as described previously (Takemori et al., 2009). The constitutively active form of SIK3 (T163E, S494A) (Katoh et al., 2006) was used in the ATDC5 cells.

### Quantitative PCR

Humeri were isolated from E18.5 embryos and tissues were crushed by vigorous shaking with beads. Total RNA was purified using an RNA purification kit (Qiagen). For cDNA synthesis, Superscript III (Invitrogen) was used according to the manufacturer's protocol. The primers used are listed in supplementary material Table S1. The PCR reaction was performed with CYBR premix reagent (TaKaRa) and the 7900HT Fast Real-Time PCR system (Applied Biosystems).

### Statistical analysis

Statistically significant differences between groups were evaluated by Student's *t*-test.  $P < 0.05$  was considered statistically significant. The analyses were performed using Excel (Microsoft) and Statcel3 (OMS Publishing).

## RESULTS

### SIK3-deficient mice have skeletal defects

Although *Sik3*<sup>-/-</sup> mice were born at the expected Mendelian frequency, 90% died on the first day after birth (T.U., Y. Itoh, O. Hatano, A. Kumagai, M. Sanosaka, T. Sasaki, S.S., J. Doi, K. Tatsumi, K. Mitamura et al., unpublished). The surviving SIK3-deficient mice showed dwarfism throughout their postnatal life. The mean weight of *Sik3*<sup>-/-</sup> mice was 7 g, whereas that of *Sik3*<sup>+/+</sup> and *Sik3*<sup>+/-</sup> mice was 13 g at 3 weeks of age. Because an X-ray analysis revealed that they had bone deformities, we focused on the skeletal abnormality as a SIK3-deficient phenotype. Anatomical examination of SIK3-deficient mice revealed numerous skeletal abnormalities (Fig. 1). When each of the skeletal elements of SIK3-deficient mice (4 months old) were compared with those of age-matched wild-type mice, we found that they had a shorter sternum

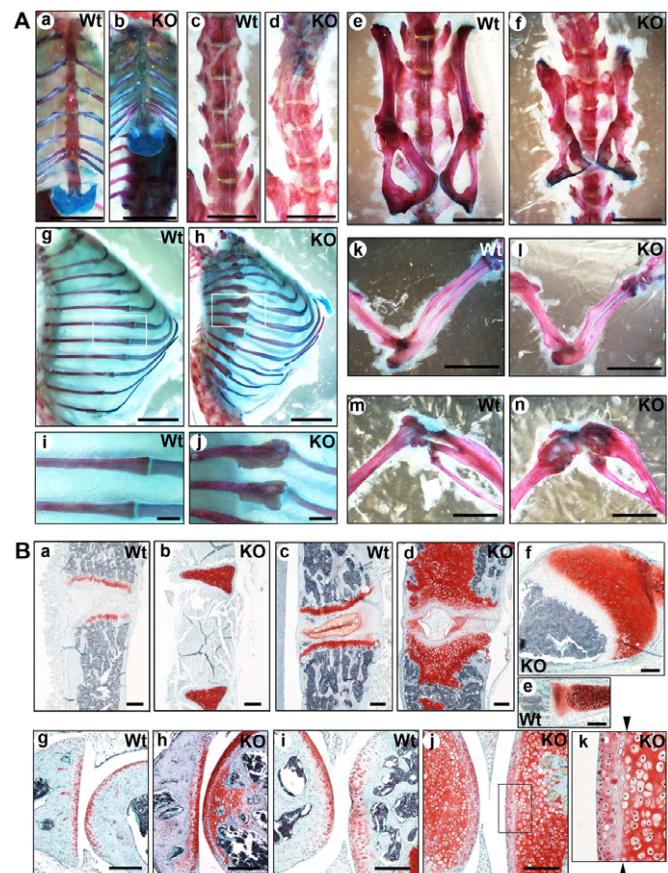


**Fig. 1. Skeletal deformity in SIK3-deficient mice. (A)** Skeletal elements from wild-type (Wt) and SIK3-deficient (KO) mice at 4 months of age stained with Alizarin Red and Alcian Blue: sternum (a,b), spine (c,d, front view), pelvis (e,f), ribcage (g,h, lateral view) and each junction (i,j), elbow (k,l) and knee (m,n). **(B)** Histological sections from wild-type and SIK3-deficient mice at 4 months of age (except for the rib junction, which was examined at 3 months of age) stained with Safranin O, Fast Green and Iron Hematoxylin: sternum (a,b), spine (c,d), rib junction (e,f), elbow (g,h) and knee (i,j), and a higher magnification view of articular cartilage regions of the knee (k). Arrowheads indicate the tide line. Scale bars: 5 mm in Aa-h; 1 mm in Ai,j; 200  $\mu$ m in B.

with low mineralization (Fig. 1Aa,b), a thinner spine that was twisted as in scoliosis (Fig. 1Ac,d), a hypoplastic pelvis (Fig. 1Ae,f), short mineralized ribs with an abnormal mass at the junction between the bone and cartilage, which was similar in appearance to a rachitic rosary (Fig. 1Ag-j), and shorter long bones (Fig. 1Ak,l) with epiphyseal and metaphyseal expansion of the limb joint region (Fig. 1Am,n). In SIK3-deficient mice, delayed membranous ossification of the skull bones was observed on postnatal day (P) 1 (supplementary material Fig. S2A,B). The parietal bone had an immature appearance from the juvenile stage until 8 months of age (supplementary material Fig. S2C-H, asterisks) and the sutures remained loosely closed throughout adulthood (supplementary material Fig. S2C-H, arrowheads). A large fontanelle remained open from juvenile stage until adulthood (supplementary material Fig. S2C-H, arrows), whereas it was already closed in 3-week-old wild-type mice. The skeletal abnormalities, especially the rachitic rosary-like structures in the ribs and unclosed large fontanelle, were reminiscent of rickets.

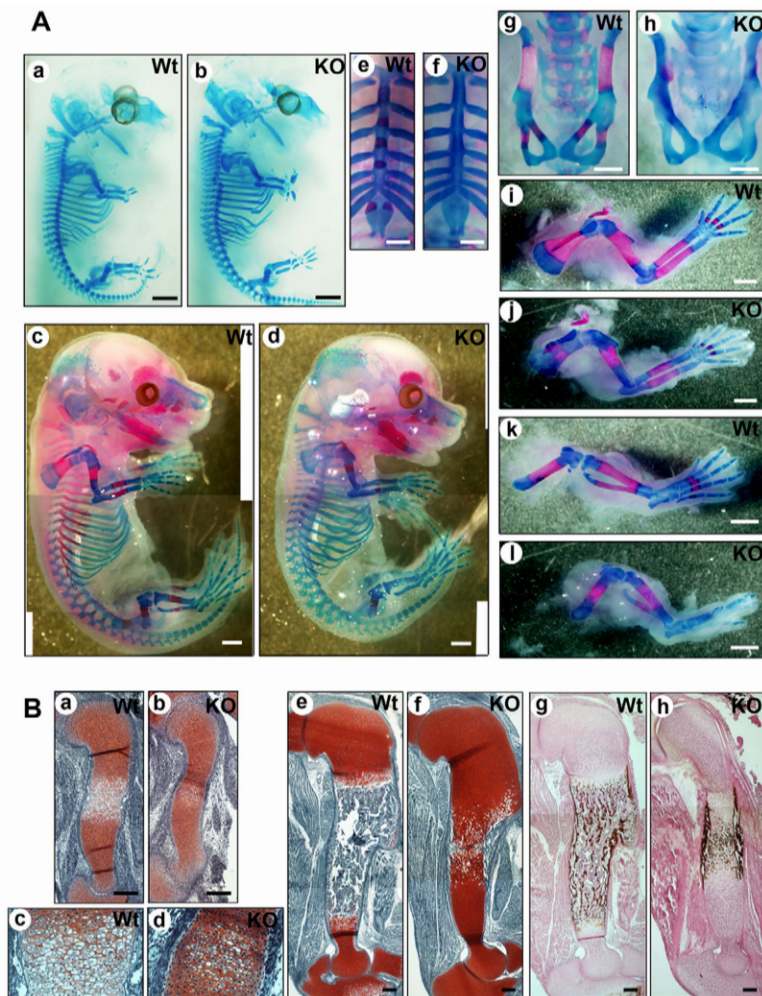


**Fig. 2. Impaired chondrocyte hypertrophy in SIK3-deficient mouse embryos.** (A) Wild-type and SIK3-deficient (KO) skeletons stained with Alizarin Red and Alcian Blue at E14.5 (a,b), E15.5 (c,d) and E18.5 (e-l): whole skeleton (a-d), sternum (e,f), pelvis (g,h), forelimb skeleton (i,j) and hindlimb skeleton (k,l). (B) Histological sections from wild-type and SIK3-deficient embryos stained with Safranin O, Fast Green and Iron Hematoxylin (a-f) or with von Kossa and Eosin (g,h) at E14.5 (a-d) and E18.5 (e-h). Scale bars: 1 mm in A; 200 μm in B.

In addition, SIK3 expression was detected in the kidney and liver, in which the effects of SIK3 deletion were also marked (T.U., Y. Itoh, O. Hatano, A. Kumagai, M. Sanosaka, T. Sasaki, S.S., J. Doi, K. Tatsumi, K. Mitamura et al., unpublished). Renal disorders produced by physical damage or chemical treatment sometimes induce osteomalacia, accompanied by low calcium and/or low phosphorus levels in the serum. Therefore, we measured the concentrations of calcium and phosphorus in the serum, and found that both were almost normal in SIK3-deficient mice (supplementary material Fig. S3). Thus, we excluded the possibility that the skeletal abnormalities of SIK3-deficient mice were due to impaired metabolism of phosphorus or calcium.

#### Accumulation of cartilage in SIK3-deficient mice

To further investigate the bone malformation in SIK3-deficient mice, we histologically analyzed the interior of the bones of 3-month-old (rib) or 4-month-old (other bones) mice. Safranin O staining revealed marked cartilage accumulation in most of the bones of SIK3-deficient mice. In the sternum, the cartilage region did not separate, and there was absolutely no bone marrow space (Fig. 1Ba,b). In the spine, expanded cartilage tissue and a malformed intervertebral disk were found (Fig. 1Bc,d). SIK3-deficient ribs were half filled with cartilage (Fig. 1Be,f). The epiphysis and metaphysis of the limb bones of SIK3-deficient mice were filled with cartilage bulk and displayed small secondary ossification centers (Fig. 1Bg-j, supplementary material Fig.

S4C,D), whereas a well-differentiated secondary ossification center was developed in wild-type mice by 3 weeks of age. Although separation between the articular cartilage and the growth plate cartilage was found in 4-month-old SIK3-deficient mice, the secondary ossification center was not well developed even by 8 months of age (supplementary material Fig. S4C-L). In the articular cartilage of SIK3-deficient mice, the zone below the tidemark was thickened. The Safranin O staining intensity and cell morphology in the zone above the tidemark of articular cartilage were similar in SIK3-deficient and wild-type mice (Fig. 1Bk). Collectively, these findings indicate that impaired chondrocyte metabolism was fundamental to the skeletal abnormalities of SIK3-deficient mice.

#### Impaired chondrocyte hypertrophy in SIK3-deficient embryos

To pinpoint the onset of the skeletal abnormalities in SIK3-deficient mice we next surveyed skeletal development at various embryonic stages by Alcian Blue/Alizarin Red staining. Neither skeletal malformation nor homeotic transformation was observed in SIK3-deficient embryos at E14.5, indicating that *Sik3* gene deletion did not affect the chondrogenic commitment of mesenchymal cells or skeletal patterning (Fig. 2Aa,b). In wild-type mouse embryos, bone mineralization was indicated by Alizarin Red staining in several skeletal elements by E15.5. Compared with wild-type embryos, delayed mineralization of the ribs, the long bones in the limbs and cervical bones was observed in SIK3-



deficient embryos at E15.5 (Fig. 2Ac,d). By E18.5, the mineralization at most skeletal elements that are developed through endochondral bone formation had progressed in wild-type embryos. By contrast, SIK3-deficient embryos displayed delayed bone mineralization. The sternum and vertebrae remained uncalcified (Fig. 2Ae-h). The mineralized regions at the pelvis (Fig. 2Ag,h), the scapula and the long bones of the forelimb and hindlimb (Fig. 2Ai-l) were markedly reduced in SIK3-deficient embryos as compared with wild-type embryos at E18.5. By contrast, the shape and size of the cartilage in the epiphyseal and metaphyseal regions of the limbs were almost normal in SIK3-deficient embryos (Fig. 2B). In spite of the reduced mineralization, the length of the long bones in the limbs was almost the same in SIK3-deficient and wild-type embryos (supplementary material Fig. S5A). Reflecting this finding, the body size of newborns was indistinguishable between genotypes (supplementary material Fig. S1C). After birth, bone elongation in the SIK3-deficient mice was restricted, and the length of the long bones in the limbs was obviously shortened at 6 weeks of age (supplementary material Fig. S5A).

A further histological analysis revealed a definitive primary defect of the cartilage in SIK3-deficient embryos. A cluster of well-differentiated hypertrophic chondrocytes is initially observed at the center of the humerus in wild-type embryos at E14.5. By contrast, only a few partially differentiated chondrocytes were observed at the center of the humerus in SIK3-deficient embryos at E14.5 (Fig. 2Ba-d). Therefore, we speculated that a disturbance of chondrocyte hypertrophy was the point at which SIK3 deficiency affected skeletal development. At E18.5, the first ossification center is well formed in the central region and the cartilage region is restricted at both ends in the wild-type mouse humerus. By contrast, the humerus of SIK3-deficient embryos was almost completely filled with cartilage tissue and the small first ossification center was barely recognizable (Fig. 2Be,f).

To characterize the cartilage tissue that accumulated in the humerus of SIK3-deficient embryos, we examined the expression of several structural markers of cartilage (types I, II and X collagen) at E18.5. We confirmed that the accumulated cartilage tissue was type I collagen-negative and type II collagen-positive, indicating that the tissue was bona fide cartilage tissue, consistent with the intense Safranin O staining (supplementary material Fig. S6A). Type X collagen, a hypertrophic structural marker, was only weakly detected at the center of the SIK3-deficient humeri, reflecting a disturbance in chondrocyte hypertrophy (supplementary material Fig. S6A). A further analysis based on cell morphology revealed that the round chondrocyte zone was of normal length but that there was an extended flat columnar chondrocyte zone and post-flat chondrocyte zone in SIK3-deficient compared with wild-type humeri at E18.5 (supplementary material Fig. S7). By assessing the expression of PCNA, it was confirmed that most of the accumulated flat chondrocytes were in a proliferative state (supplementary material Fig. S8).

In spite of the disruption of chondrocyte hypertrophy, significant mineralization, as confirmed by von Kossa staining, was observed at the bone collar of the humerus in SIK3-deficient embryos at E18.5, and it was apparently thicker than that in wild-type embryos (Fig. 2Bg,h). A real-time RT-PCR analysis showed that the genes encoding the mineralization factors ANK and ENPP were expressed at E18.5 in SIK3-deficient humerus, although the expression levels were slightly reduced (supplementary material Fig. S5B). The expression levels of the genes encoding the vascularization factors VEGF and VEGFR

and the hypoxia inducible factors HIF1 $\alpha$  and HIF2 $\alpha$  (EPAS1 – Mouse Genome Informatics) were similar in wild-type and SIK3-deficient humeri (supplementary material Fig. S5B). A similar phenomenon has been reported in *Sox9* transgenic embryos, in which chondrocyte hypertrophy was suppressed (Akiyama et al., 2004; Hattori et al., 2010). These findings suggest that there is a system that compensates for bone mineralization in cases of disruption of endochondral skeletal development. We also performed the TUNEL assay to determine whether apoptosis was occurring in the accumulating cartilage tissue in SIK3-deficient embryos and juvenile mice. Few TUNEL-positive cells were detected in the accumulating cartilage tissue of E18.5 and juvenile specimens (supplementary material Fig. S8), suggesting that the accumulated chondrocytes in SIK3-deficient mice were not actively removed but remain alive until entry into hypertrophy upon differentiation.

Although the SIK3-deficient humerus was filled with chondrocytes at E18.5 (Fig. 2Be,f), first and secondary ossification centers were eventually formed (supplementary material Fig. S4) and mineralization occurred (Fig. 1A) with increasing age. These results suggested that the chondrocyte hypertrophy program was diminished rather than completely abolished. In order to clarify whether the post-hypertrophic program was still functional, we analyzed the expression of MMP13, a post-hypertrophic marker (Mitchell et al., 1996), and of SP7 (osterix), an osteogenesis marker (Nakashima et al., 2002), in juvenile epiphyseal tibia specimens. Consistently, expression of these markers was observed, although their expression patterns were somewhat disorganized compared with the wild-type tissues (supplementary material Fig. S6B). Taken together, it was concluded that the major effect of SIK3 deficiency on skeletal development was disruption of chondrocyte hypertrophy.

### Expression of SIK3 in hypertrophic chondrocytes

Based on a histological analysis, we revealed that SIK3 deficiency results in the disruption of chondrocyte hypertrophy (Figs 1, 2). To address the endogenous SIK3 expression pattern in cartilage tissue, we performed immunofluorescent staining for SIK3 in wild type. Consistent with the histological results, endogenous SIK3 was detected in both prehypertrophic and hypertrophic chondrocytes, and it was localized in the cytoplasm of cells in the humerus at E18.5 (Fig. 3Aa,b), scapula at E15.5 (Fig. 3Ac,d) and growth plate of the knee at 3 weeks of age (Fig. 3Ae,f).

Previously, it was revealed that HDAC4 and MEF2C are central regulators of chondrocyte hypertrophy and skeletogenesis and that HDAC4 functions as a transcriptional repressor for MEF2C and RUNX2 (Vega et al., 2004; Arnold et al., 2007). Other studies have also reported interactions between SIK1/2 and HDACs (van der Linden et al., 2007; Takemori et al., 2009). We therefore hypothesized that SIK3 might exert its effect via HDAC4 to regulate the activities of MEF2C and RUNX2 in chondrocyte hypertrophy. To evaluate this hypothesis, we first immunohistochemically analyzed the expression of SOX9, HDAC4 and MEF2C (as a representative target of HDAC4) in the wild-type humerus at E15.5 (Fig. 3B). As previously reported, SOX9 was detected in the proliferative and in some of the prehypertrophic chondrocytes and was undetectable in hypertrophic chondrocytes (Fig. 3Bc,d). Expression of MEF2C and HDAC4 was detected in both the prehypertrophic and hypertrophic chondrocyte regions (Fig. 3Be-h). The expression of SIK3 was exclusive to cells that also expressed SOX9 and was similar to that of HDAC4 (Fig. 3Bi,j).

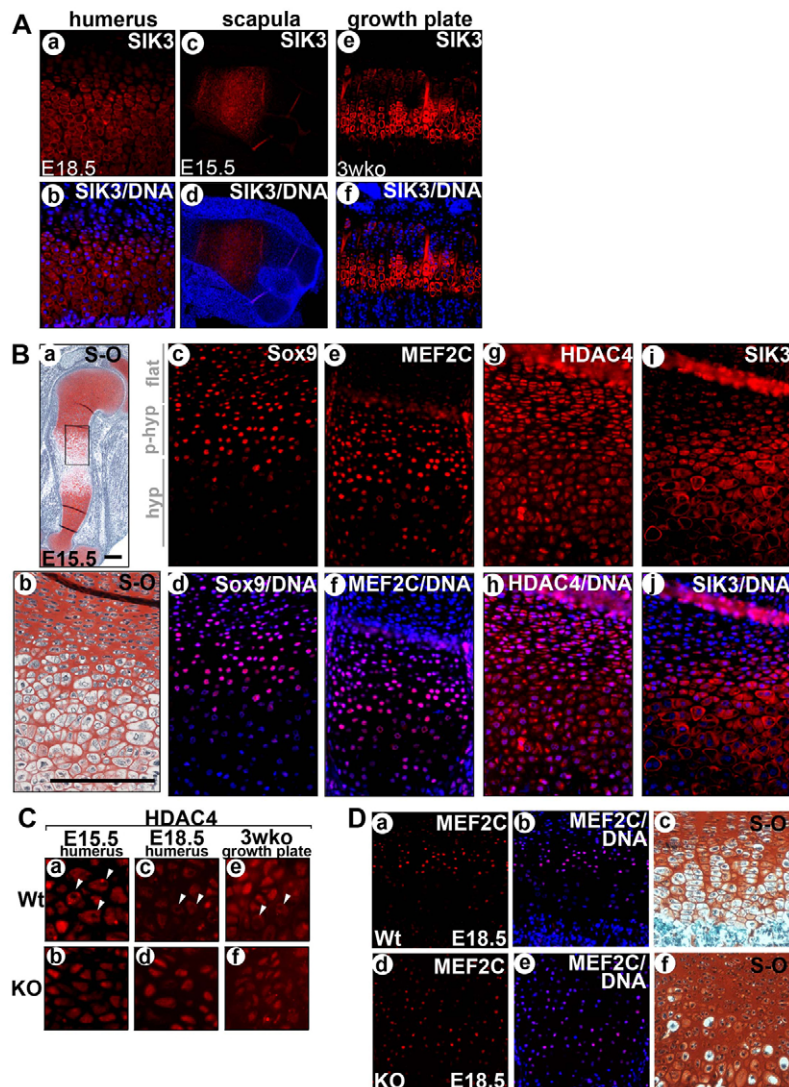


**Fig. 3. Expression patterns of SIK3 and chondrocyte hypertrophic factors.** (A) Immunofluorescent staining for SIK3 (red) in the humerus (a,b), scapula (c,d) and growth plate of the proximal tibia of 3-week-old (e,f) wild-type mice. Nuclei were counterstained with Hoechst 33342 (blue). SIK3 expression was detected in prehypertrophic and hypertrophic chondrocytes and was localized in the cytoplasm in all tissues analyzed. (B) A comparison of the expression patterns of SIK3 and chondrocyte hypertrophic factors in the humerus of wild-type embryos (E15.5). Bright-field views of a section stained with Safranin O, Fast Green and Hematoxylin are shown (a,b). Serial sections were stained with anti-SOX9 (c,d), anti-MEF2C (e,f), anti-HDAC4 (g,h) or anti-SIK3 (i,j) antibodies and an Alexa Fluor-conjugated secondary antibody. Scale bars: 200  $\mu$ m. (C) Immunofluorescent staining for HDAC4 in the humerus at E15.5 (a,b) and E18.5 (c,d) and in the growth plate of the proximal tibia at 3 weeks of age (e,f) of wild-type (a,c,e) and SIK3-deficient (b,d,f) mice. Arrowheads indicate cells in which HDAC4 was excluded from the nucleus. However, HDAC4 persisted in the nucleus in the SIK3-deficient specimens. (D) Immunofluorescent staining for MEF2C in the humerus at E18.5 in wild-type (a,b) and SIK3-deficient (d,e) embryos. Semi-serial sections were stained with Safranin O, Fast Green and Hematoxylin (c,f).

We also found that there was a shift in the subcellular localization of HDAC4 to the cytoplasm in hypertrophic chondrocytes, where the expression of MEF2C was strong in the nuclei. The translocation of HDAC4 was observed at the hypertrophic chondrocyte zone in the humerus of E15.5 and E18.5 embryos and in the growth plate of 3-week-old wild-type mice (Fig. 3C). By contrast, HDAC4 translocation to the cytoplasm was seldom observed in chondrocytes at the corresponding region in SIK3-deficient embryos and mice. However, although the location was not synchronized, significant MEF2C-positive cells were observed at the edge of the accumulated cartilage in SIK3-deficient humeri, despite the fact that chondrocyte hypertrophy had not progressed (Fig. 3Dd-f). We therefore concluded that the HDAC4 remaining in the nuclei of the SIK3-deficient chondrocytes continued to repress MEF2C activity, resulting in the blockage of chondrocyte hypertrophy. Taken together, these data indicated that SIK3 is required for HDAC4 translocation to the cytoplasm during chondrocyte hypertrophy.

### SIK3 forms a complex with HDAC4 to regulate its subcellular localization

To address how SIK3 regulates the subcellular localization of HDAC4, we performed a co-immunoprecipitation assay to determine whether they form a complex. The co-

immunoprecipitation assay with knee lysates from 2-week-old mice indicated that a complex was indeed formed between HDAC4 and SIK3 (Fig. 4A). To further analyze the regulation of HDAC4 by SIK3 in vitro, HA-tagged HDAC4 and SIK3 expression vectors were co-transfected into 293FT cells, lysed, and assayed with an anti-HA antibody. This confirmed that HDAC4 and SIK3 form a complex (Fig. 4B). Using this system, we explored the binding domains of SIK3 and HDAC4 required for complex formation, and identified the kinase domain (amino acids 1-270) of SIK3 and the central region (amino acids 351-620) of HDAC4 as binding domains (supplementary material Fig. S9).

We next examined whether this interaction affects the subcellular localization of HDAC4. To monitor HDAC4 localization, an EGFP-tagged HDAC4 expression vector was transfected into 293FT cells with or without the SIK3 expression vector, and GFP was observed by fluorescence microscopy. In agreement with the expression pattern of endogenous SIK3 in hypertrophic chondrocytes (Fig. 3B), the overexpressed SIK3 was detected in the cytoplasm (Fig. 4C). When GFP-HDAC4 was overexpressed alone, GFP fluorescence was observed in the nucleus (Fig. 4D, upper panel). By contrast, when SIK3 was co-expressed, GFP fluorescence was observed in the cytoplasm (Fig. 4D, bottom panels). These results indicated that SIK3 can alter the localization

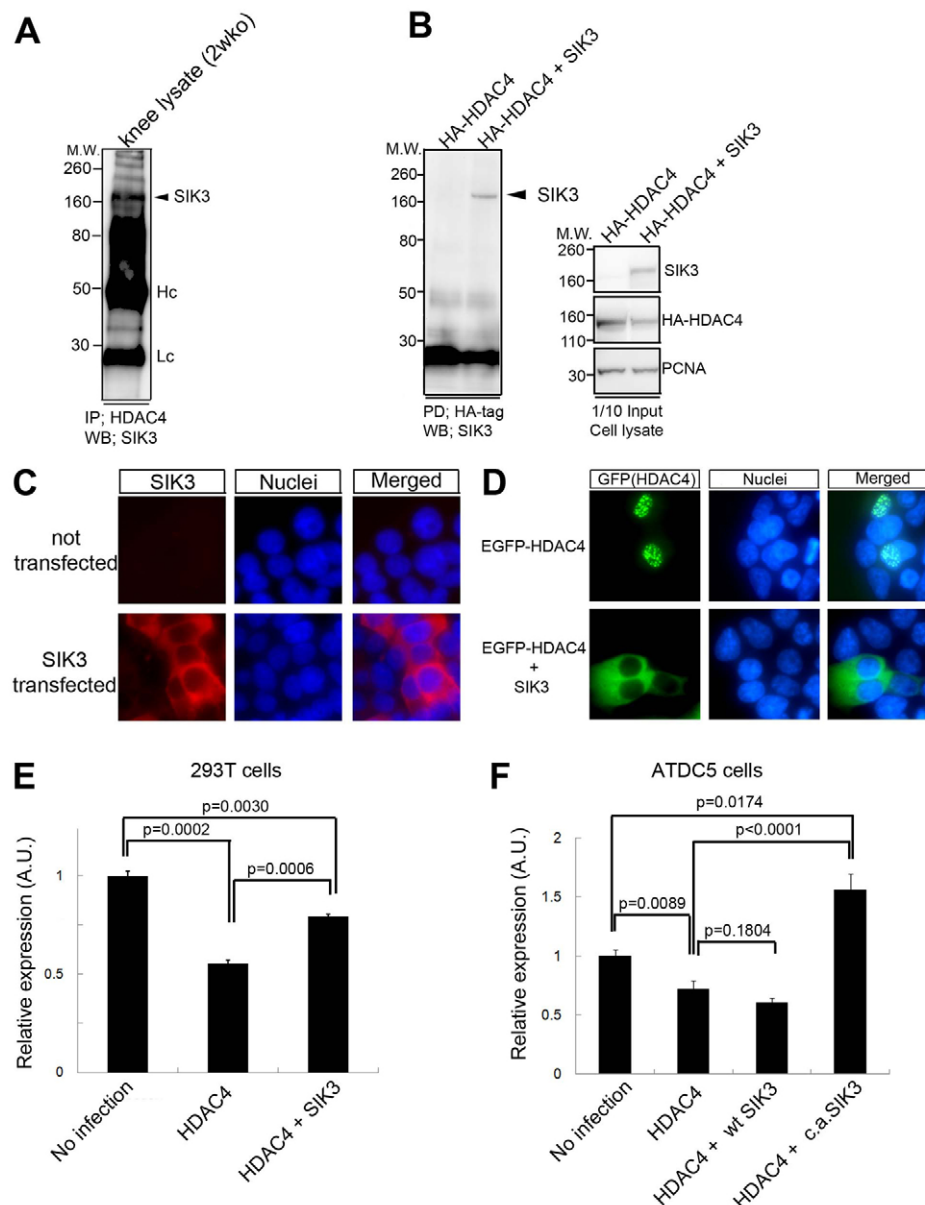


**Fig. 4. Interaction of SIK3 with HDAC4 regulates its subcellular localization.** (A) Co-immunoprecipitation of SIK3 with HDAC4. Knee tissue from 2-week-old mice was lysed and endogenous HDAC4 immunoprecipitated. Co-immunoprecipitated SIK3 was detected. Hc, IgG heavy chain; Lc, IgG light chain. (B) Pull-down assay of SIK3 with HA-HDAC4. 293FT cells were transiently transfected with expression vectors carrying SIK3 and HA-tagged HDAC4. Pulled-down samples (PD) and whole cell lysates (input) were subjected to SDS-PAGE followed by immunoblotting with the indicated antibodies. Left and right panels show the pull-down assay and the transiently expressed proteins, respectively. PCNA was monitored as a loading control. (C) SIK3 immunofluorescence. 293FT cells were transiently transfected with a SIK3 expression vector and stained 24 hours after transfection using an anti-SIK3 antibody followed by an Alexa Fluor-conjugated secondary antibody. A SIK3 signal was detected in the cytoplasm of transfected cells, whereas there was no substantial signal in non-transfected cells. (D) Translocation of HDAC4 by SIK3. A GFP-HDAC4 expression vector was transfected with or without a SIK3 expression vector into 293FT cells. When EGFP-HDAC4 was transfected alone, GFP fluorescence was detected in the nuclei (top panels). When EGFP-HDAC4 and SIK3 were co-transfected, GFP fluorescence was detected in the cytoplasm (bottom panels). Nuclei were counterstained with Hoechst 33342. (E) MEF2C transcriptional activity in 293FT cells. 293FT cells were transiently transfected with a MEF2C-luciferase reporter plasmid and an expression vector encoding MEF2C without (basal control) or with expression vectors for HDAC4 and/or wild-type SIK3. The luciferase activity was measured 48 hours after transfection. (F) MEF2C transcriptional activity in ATDC5 cells. ATDC5 cells were transiently transfected with a MEF2C-luciferase reporter plasmid and an expression vector encoding MEF2C without (basal control) or with expression vectors for HDAC4 and/or wild-type SIK3, or with a constitutively active form of SIK3 (T163E, S494A). Error bars indicate s.d.

of HDAC4 from the nucleus to the cytoplasm. We also performed a MEF2C luciferase reporter assay to monitor whether the HDAC4 translocation induced by SIK3 might relieve MEF2C activity from suppression by HDAC4. When MEF2C was co-expressed with HDAC4, the MEF2C reporter activity was suppressed. In addition,

when SIK3 was co-overexpressed recovery of the luciferase activity was observed, although the recovery was not complete (Fig. 4E). In ATDC5 cells, a prechondrogenic cell line, constitutively active forms of SIK3 (T163E, S494A), but not wild-type SIK3, showed HDAC4 inhibitory activity, suggesting that



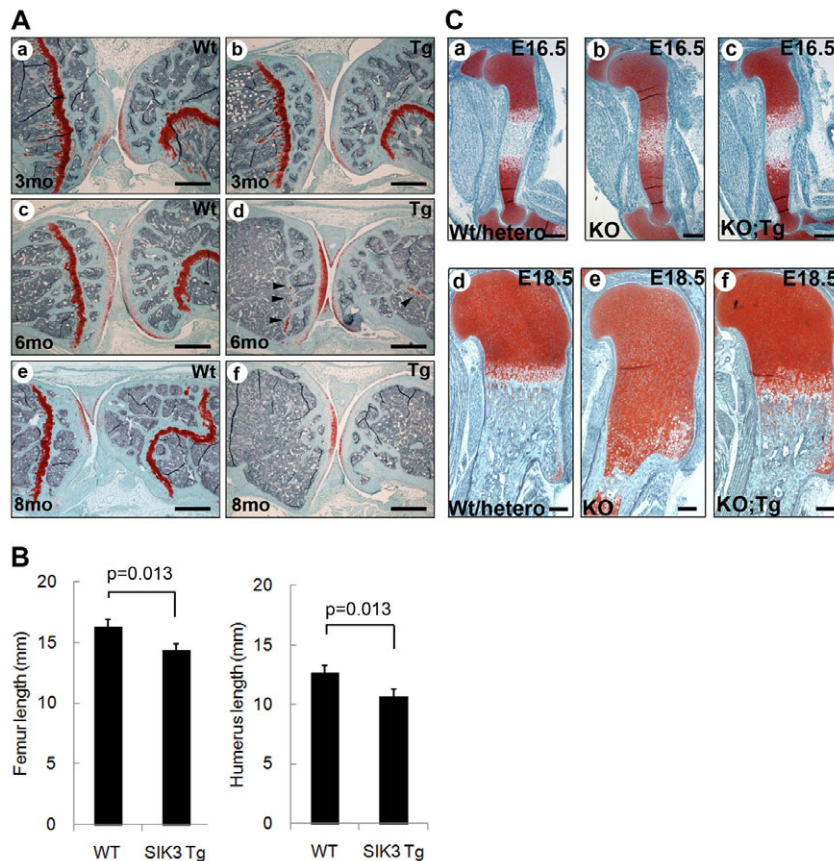


**Fig. 5. Effects of forced expression of SIK3 in cartilage tissue.** (A) Histological sections of the knee joint of wild-type and *Col11a2-hSIK3* transgenic mice stained with Safranin O and Fast Green. At 3 months of age, the growth plate of the transgenic mice appeared normal (a,b). By 6 months, the growth plate was starting to disappear (c,d) and by 8 months of age it had completely disappeared and the spongy bone was also starting to disappear (e,f). By contrast, the growth plates persisted in wild-type mice until they were 8 months of age. Arrowheads indicate the residual growth plates. (B) A comparison of the length of femur and humerus between wild-type and *hSIK3* transgenic (Tg) mice at 6 months of age. The *hSIK3* transgenic mice had shortened long bones. Error bars indicate s.d. (C) Transgenic rescue of SIK3. A *SiK3*<sup>-/-</sup> female mouse was mated with a *SiK3*<sup>-/-</sup>; *Col11a2-hSIK3* transgenic male mouse and the embryos were dissected at E16.5 (a-c) or E18.5 (d-f). Chondrocyte accumulation in the SIK3-deficient proximal humerus was substantially restored by the *Col11a2-hSIK3* transgene. Scale bars: 500  $\mu$ m in A; 200  $\mu$ m in C.

ATDC5 cells lack factors that are required for the activation of SIK3 (Fig. 4F). Overall, these findings indicated that SIK3 anchors HDAC4 in the cytoplasm, thereby allowing MEF2C to be active.

### Forced SIK3 expression in cartilage causes closure of the growth plate in adulthood

The expression of SIK3 in hypertrophic chondrocytes and impaired chondrocyte hypertrophy in SIK3-deficient embryos and mice indicate that SIK3 is indispensable for chondrocyte hypertrophy. We generated transgenic mice overexpressing human *SIK3* (*hSIK3*) specifically in chondrocytes under the control of *Col11a2* promoter/enhancer sequences (Tsumaki et al., 1996; Murai et al., 2008; Hiramatsu et al., 2011) to confirm the role of SIK3 in cartilage by a gain-of-function approach and to clarify that the phenotype of bone malformation in SIK3-deficient mice was really due to the cartilage tissue.

We previously demonstrated that GFP fluorescence driven by this system is detected only in the cartilage tissue during embryogenesis (Hiramatsu et al., 2011) and in both the articular and growth plate cartilage in adulthood (data not shown). To confirm the expression of the *hSIK3* transgene using this system, costal cartilage was harvested from postnatal pups at the P2 stage and subjected to SDS-PAGE, followed by immunoblotting with a SIK3 antibody (supplementary material Fig. S10). Although a dramatic effect of SIK3 overexpression was not observed during embryogenesis or during the juvenile period in *Col11a2-hSIK3* transgenic mice, we did observe the disappearance of the growth plate in the hind limbs with aging (Fig. 5A).

Generally, the growth plate is thought to comprise continually metabolizing chondrocytes, which are balanced in proliferation and differentiation (i.e. hypertrophy). Based on our findings, we

speculated that the disappearance of the growth plate in cartilage-specific *hSIK3* transgenic mice occurred because the overexpressed SIK3 slightly accelerated the differentiation of chondrocytes at the growth plate, leading to chronic and excessive usage of chondrocytes and resulting in loss of the growth plate structure in older mice. Consistent with this hypothesis, the length of the long bones was reduced at 6 months of age (Fig. 5B) and the spongy bone structure was also beginning to disappear by 8 months of age in the *Col11a2-hSIK3* transgenic mice (Fig. 5A). Thus, we concluded that the disappearance of the growth plate in cartilage-specific *hSIK3* transgenic mice was a predictable phenotype for the gain-of-function approach for SIK3. In addition, the *Col11a2-hSIK3* transgenic/SIK3-deficient offspring displayed efficient rescue of the impaired chondrocyte hypertrophy phenotype at E16.5 (Fig. 5C, top panels) and at E18.5 (Fig. 5C, bottom panels). Nevertheless, despite the restoration of the bone phenotype, the lethality of SIK3 deficiency for newborn mice was not recovered, suggesting that bone deformity is not the primary cause of their postnatal death. Taken together, these results confirmed that the role of SIK3 in chondrocytes is to induce the progression of chondrocyte hypertrophy and that the impaired skeletal development of SIK3-deficient mice is due to the cartilage tissue.

### DISCUSSION

Our study revealed that SIK3 is a crucial regulator of chondrocyte hypertrophy and identified the transcriptional regulator, HDAC4, as a target of SIK3 in chondrogenesis. SIK3-deficient mice displayed multiple phenotypes, including bone malformation with dwarfism, and these were concluded to be due to impaired chondrocyte hypertrophy. The abnormalities of the bone that develops via endochondral bone formation in



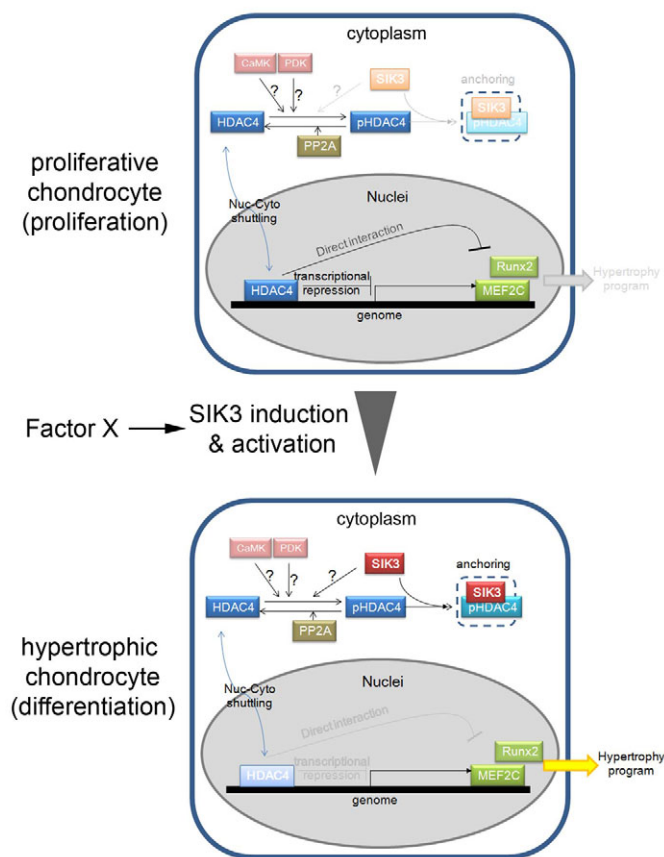


**Fig. 6. Model depicting the role of SIK3 in chondrocyte hypertrophy.** (Top) When SIK3 is absent, HDAC4 remains in the nucleus and epigenetically and mechanically represses MEF2C. (Bottom) Once SIK3 is induced, SIK3 binds to HDAC4 and anchors it in the cytoplasm, thereby allowing MEF2C to become active in the nucleus and facilitating the progression of the chondrocyte hypertrophic program. Question marks indicate possible phosphorylation activities opposing to PP2A, but not tested.

SIK3-deficient embryos were similar to those of cartilage-specific *Hdac4* transgenic embryos (Vega et al., 2004). Furthermore, our results showed that SIK3 forms a complex with HDAC4 and anchors it in the cytoplasm, thereby relieving MEF2C from transcriptional repression by HDAC4 in the nuclei. In conclusion, the regulation of HDAC4 by SIK3 is a crucial mechanism for the progression of chondrocyte hypertrophy during skeletal development (Fig. 6).

### Expression of SIK3 in chondrocytes

SIK3-deficient mice were generated to better understand the physiological role of SIK3. We identified bone deformity with dwarfism as one of the phenotypes of SIK3-deficient mice. We found strong expression of SIK3 from prehypertrophic to hypertrophic chondrocytes during chondrogenesis and in the postnatal growth plate, suggesting the importance of SIK3 in chondrocyte hypertrophy. Indeed, SIK3-deficient embryos displayed impaired chondrocyte hypertrophy, which resulted in bone abnormalities. Furthermore, cartilage-specific *hSIK3* transgenic mice showed unnatural closure of the growth plate. As a result of our gain-of-function approach, it was demonstrated that the expression of additional SIK3 hastened chondrocyte hypertrophy and led to the depletion of non-hypertrophic

chondrocytes, which are normally necessary to maintain the growth plate structure. Although the SIK3 expression pattern was consistent with its function in chondrocytes, further questions also arose. For example, it is unclear how and which transcription factor(s) regulate SIK3 expression in chondrocytes. So far, there have been few studies, but we intend to address this question in future studies to obtain a deeper understanding of the mechanism responsible for endochondral bone development.

### Molecular mechanisms by which SIK3 exerts its activity in chondrocytes

One of the major findings of this study is that SIK3 regulates the subcellular localization of HDAC4, a negative transcriptional regulator of MEF2C and RUNX2 activity during chondrocyte differentiation, i.e. hypertrophy. For the first time, we revealed that SIK3 was strongly expressed from prehypertrophic to hypertrophic chondrocytes, in which HDAC4 was also expressed. In addition, we found that HDAC4 localization was shifted to the cytoplasm in wild-type chondrocytes, but that this seldom occurred in SIK3-deficient chondrocytes. In response to HDAC4 translocation, wild-type chondrocytes began hypertrophy. By contrast, chondrocyte hypertrophy was severely inhibited in spite of sufficient MEF2C expression in SIK3-deficient cartilage tissue. However, flat chondrocytes continued proliferating, maintaining their columnar structure and causing chondrocyte accumulation during development. These results suggested that SIK3 is required for proper chondrocyte hypertrophy and that its role is to change the subcellular localization of HDAC4 from the nucleus to the cytoplasm during chondrocyte differentiation.

Several studies have reported that SIK1 and SIK2 directly regulate HDACs (van der Linden et al., 2007; Takemori et al., 2009). Fly SIK3 (the homolog of mouse SIK2) has recently been shown to sequester HDAC4 in the cytoplasm and to regulate the energy balance in the *Drosophila* fat body (Wang et al., 2011). We therefore hypothesized that mouse SIK3 directly regulates HDAC4. Indeed, we confirmed that SIK3 and HDAC4 form a stable complex by performing a pulldown assay. We found that the subcellular localization of SIK3 in chondrocytes *in vivo* was the cytoplasm. In fact, we did not find any nuclear localization signal in its sequence, and the SIK3 that was ectopically expressed in the 293FT cells was detected in the cytoplasm. By contrast, HDAC4 was detected in both the cytoplasm and the nucleus in proliferative chondrocytes, whereas it was localized in the cytoplasm in hypertrophic chondrocytes. It is also known that HDAC4 shuttles between the cytoplasm and nucleus. Considering these findings, it appears that when SIK3 is present in the cytoplasm, HDAC4 is anchored there. Consistent with this idea, we demonstrated that GFP-HDAC4, which was localized in nuclei when expressed alone, was localized in the cytoplasm when SIK3 was co-expressed in 293FT cells. Furthermore, anchoring HDAC4 to the cytoplasm by SIK3 co-expression allowed reactivation of the MEF2C repressed by HDAC4 in nuclei *in vitro*.

It is thought that the role of SIK3 during chondrocyte differentiation is to exclude HDAC4 from the nucleus, thereby allowing MEF2C to be transcriptionally active in the nucleus to induce progression of the chondrocyte hypertrophy program. We found that constitutively active forms of SIK3 (T163E, S494A), but not wild-type SIK3, inhibited HDAC4 activity in ATDC5 cells, suggesting the presence of other factors that are needed for SIK3 activation. Previously, LKB1 (STK11 – Mouse Genome

Informatics) was shown to be an activator of SIK3, and it phosphorylates SIK3 at Thr163 (Lizcano et al., 2004), raising the possibility that LKB1 might be a regulator of SIK3. The mild cartilage phenotype in *Col11a2-hSIK3* transgenic mice compared with that in *Mef2c* transgenic or HDAC4-deficient mice might indicate that the presence of additional factors is required for the activation of *Sik3* in chondrocytes. In the *hSIK3* transgenic growth plate, we did not see obvious changes in HDAC4 localization (data not shown) in spite of the presence of growth plate abnormalities. A possible explanation for this discrepancy is that the changes might have been too faint to be detected by immunofluorescence microscopy. It is also possible that other undefined mechanisms act downstream of SIK3, in parallel to HDAC4. *Col11a2-hSIK3* transgenic mice showed early closure of the growth plates. Growth plate disappearance has been reported in mice in which IHH (Maeda et al., 2007) and the PTH/PTHrP receptor (Hirai et al., 2011) were deleted postnatally. Because IHH and PTH/PTHrP regulate chondrocyte hypertrophy, SIK3 might be localized and controlled by these signaling molecules during the progression of chondrocyte hypertrophy. The SIK3-deficient cartilage phenotype was rescued by *Col11a2-hSIK3* transgene expression, suggesting that the impaired skeletal development in SIK3-deficient mice is primarily due to the cartilage tissue. It is also possible that changes in cholesterol metabolism and malnourishment phenotypes in the SIK3-deficient mice (T.U., Y. Itoh, O. Hatano, A. Kumagai, M. Sanosaka, T. Sasaki, S.S., J. Doi, K. Tatsumi, K. Mitamura et al., unpublished) affect chondrocyte differentiation, as cholesterol signaling stimulates chondrocyte hypertrophy (Woods et al., 2009) and because malnourishment phenotypes, including lipodystrophy, hypolipidemia and hypoglycemia, should affect skeletal growth. The SIK3-deficient bone phenotypes displayed at adulthood in this study might have occurred due to a combination of direct SIK3 disruption in chondrocytes and indirect SIK3 disruption due to metabolic changes.

Previously, PP2A was proposed as a regulator of HDAC4 by localizing it in the nucleus, thereby prohibiting chondrocyte hypertrophy (Kozhemyakina et al., 2009). However, no opposing mechanisms have been suggested. Our present findings are therefore the first to indicate that SIK3 has an antagonistic role in HDAC4 regulation during chondrogenesis. Although we did not perform an in-depth analysis of the underlying mechanism(s) of action in this study, we did observe impaired skull bone development, which occurs through membranous ossification, suggesting that SIK3 is involved in membranous ossification as well. Further studies are needed to better understand the functions of SIK3 in skeletal development, including the generation of conditional knockout mice.

#### Acknowledgements

We thank Dr Gen Nishimura for advice on manuscript preparation; Dr James Hsieh for providing instructions for the immunoprecipitation assay; Ms Mari Shinkawa for technical assistance; Drs Hidetatsu Outani, Hirohiko Yasui, Yoshiki Minogishi, Minoru Okada, Jun Yoshino and Takao Hirai for discussions and suggestions; and Dr Kazuyuki Itoh for support.

#### Funding

This study was supported in part by the Japan Science Technology Agency (JST); Core Research for Evolutional Science and Technology (CREST) (to N.T.); Ministry of Education, Culture, Sports, Science and Technology (MEXT) [Scientific Research Grant No. 21390421 to N.T.]; and the Natural Scientists and the Strategic Project to Support the Formation of Research Bases at Private Universities (to H.T.).

#### Competing interests statement

The authors declare no competing financial interests.

#### Supplementary material

Supplementary material available online at <http://dev.biologists.org/lookup/suppl/doi:10.1242/dev.072652/-DC1>

#### References

- Akiyama, H., Chaboissier, M. C., Martin, J. F., Schedl, A. and de Crombrughe, B. (2002). The transcription factor Sox9 has essential roles in successive steps of the chondrocyte differentiation pathway and is required for expression of Sox5 and Sox6. *Genes Dev.* **16**, 2813-2828.
- Akiyama, H., Lyons, J. P., Mori-Akiyama, Y., Yang, X., Zhang, R., Zhang, Z., Deng, J. M., Taketo, M. M., Nakamura, T., Behringer, R. R. et al. (2004). Interactions between Sox9 and beta-catenin control chondrocyte differentiation. *Genes Dev.* **18**, 1072-1087.
- Arnold, M. A., Kim, Y., Czubyrt, M. P., Phan, D., McAnally, J., Qi, X., Shelton, J. M., Richardson, J. A., Bassel-Duby, R. and Olson, E. N. (2007). MEF2C transcription factor controls chondrocyte hypertrophy and bone development. *Dev. Cell* **12**, 377-389.
- Hattori, T., Muller, C., Gebhard, S., Bauer, E., Pausch, F., Schlund, B., Bosl, M. R., Hess, A., Surmann-Schmitt, C., von der Mark, H. et al. (2010). SOX9 is a major negative regulator of cartilage vascularization, bone marrow formation and endochondral ossification. *Development* **137**, 901-911.
- Hirai, T., Chagin, A. S., Kobayashi, T., Mackem, S. and Kronenberg, H. M. (2011). Parathyroid hormone/parathyroid hormone-related protein receptor signaling is required for maintenance of the growth plate in postnatal life. *Proc. Natl. Acad. Sci. USA* **108**, 191-196.
- Hiramatsu, K., Sasagawa, S., Outani, H., Nakagawa, K., Yoshikawa, H. and Tsumaki, N. (2011). Generation of hyaline cartilaginous tissue from mouse adult dermal fibroblast culture by defined factors. *J. Clin. Invest.* **121**, 640-657.
- Ikegami, D., Akiyama, H., Suzuki, A., Nakamura, T., Nakano, T., Yoshikawa, H. and Tsumaki, N. (2011). Sox9 sustains chondrocyte survival and hypertrophy in part through PI3K-Akt pathways. *Development* **138**, 1507-1519.
- Karsenty, G., Kronenberg, H. M. and Settembre, C. (2009). Genetic control of bone formation. *Annu. Rev. Cell Dev. Biol.* **25**, 629-648.
- Katoh, Y., Takemori, H., Horike, N., Doi, J., Muraoka, M., Min, L. and Okamoto, M. (2004). Salt-inducible kinase (SIK) isoforms: their involvement in steroidogenesis and adipogenesis. *Mol. Cell. Endocrinol.* **217**, 109-112.
- Katoh, Y., Takemori, H., Lin, X. Z., Tamura, M., Muraoka, M., Satoh, T., Tsuchiya, Y., Min, L., Doi, J., Miyauchi, A. et al. (2006). Silencing the constitutive active transcription factor CREB by the LKB1-SIK signaling cascade. *FEBS J.* **273**, 2730-2748.
- Komori, T., Yagi, H., Nomura, S., Yamaguchi, A., Sasaki, K., Deguchi, K., Shimizu, Y., Bronson, R. T., Gao, Y. H., Inada, M. et al. (1997). Targeted disruption of *Cbfa1* results in a complete lack of bone formation owing to maturational arrest of osteoblasts. *Cell* **89**, 755-764.
- Kozhemyakina, E., Cohen, T., Yao, T. P. and Lassar, A. B. (2009). Parathyroid hormone-related peptide represses chondrocyte hypertrophy through a protein phosphatase 2A/histone deacetylase 4/MEF2 pathway. *Mol. Cell. Biol.* **29**, 5751-5762.
- Lefebvre, V. and Smits, P. (2005). Transcriptional control of chondrocyte fate and differentiation. *Birth Defects Res. C Embryo Today* **75**, 200-212.
- Lizcano, J. M., Goransson, O., Toth, R., Deak, M., Morrice, N. A., Boudeau, J., Hawley, S. A., Udd, L., Makela, T. P., Hardie, D. G. et al. (2004). LKB1 is a master kinase that activates 13 kinases of the AMPK subfamily, including MARK/PAR-1. *EMBO J.* **23**, 833-843.
- Maeda, Y., Nakamura, E., Nguyen, M. T., Suva, L. J., Swain, F. L., Razzaque, M. S., Mackem, S. and Lanske, B. (2007). Indian Hedgehog produced by postnatal chondrocytes is essential for maintaining a growth plate and trabecular bone. *Proc. Natl. Acad. Sci. USA* **104**, 6382-6387.
- Mitchell, P. G., Magna, H. A., Reeves, L. M., Lopresti-Morrow, L. L., Yocum, S. A., Rosner, P. J., Geoghegan, K. F. and Hambor, J. E. (1996). Cloning, expression, and type II collagenolytic activity of matrix metalloproteinase-13 from human osteoarthritic cartilage. *J. Clin. Invest.* **97**, 761-768.
- Murai, J., Ikegami, D., Okamoto, M., Yoshikawa, H. and Tsumaki, N. (2008). Insulation of the ubiquitous Rxb promoter from the cartilage-specific adjacent gene, *Col11a2*. *J. Biol. Chem.* **283**, 27677-27687.
- Nakashima, K., Zhou, X., Kunkel, G., Zhang, Z., Deng, J. M., Behringer, R. R. and de Crombrughe, B. (2002). The novel zinc finger-containing transcription factor *ostx1* is required for osteoblast differentiation and bone formation. *Cell* **108**, 17-29.
- Ng, L. J., Wheatley, S., Muscat, G. E., Conway-Campbell, J., Bowles, J., Wright, E., Bell, D. M., Tam, P. P., Cheah, K. S. and Koopman, P. (1997). SOX9 binds DNA, activates transcription, and coexpresses with type II collagen during chondrogenesis in the mouse. *Dev. Biol.* **183**, 108-121.
- Olsen, B. R., Reginato, A. M. and Wang, W. (2000). Bone development. *Annu. Rev. Cell Dev. Biol.* **16**, 191-220.



- Takeda, S., Bonnamy, J. P., Owen, M. J., Ducy, P. and Karsenty, G.** (2001). Continuous expression of Cbfa1 in nonhypertrophic chondrocytes uncovers its ability to induce hypertrophic chondrocyte differentiation and partially rescues Cbfa1-deficient mice. *Genes Dev.* **15**, 467-481.
- Takeda, S., Chen, D. Y., Westergard, T. D., Fisher, J. K., Rubens, J. A., Sasagawa, S., Kan, J. T., Korsmeyer, S. J., Cheng, E. H. and Hsieh, J. J.** (2006). Proteolysis of MLL family proteins is essential for caspase-1-orchestrated cell cycle progression. *Genes Dev.* **20**, 2397-2409.
- Takemori, H., Katoh Hashimoto, Y., Nakae, J., Olson, E. N. and Okamoto, M.** (2009). Inactivation of HDAC5 by SIK1 in AICAR-treated C2C12 myoblasts. *Endocrine J.* **56**, 121-130.
- Tsumaki, N., Kimura, T., Matsui, Y., Nakata, K. and Ochi, T.** (1996). Separable cis-regulatory elements that contribute to tissue- and site-specific alpha 2(XI) collagen gene expression in the embryonic mouse cartilage. *J. Cell Biol.* **134**, 1573-1582.
- van der Linden, A. M., Nolan, K. M. and Sengupta, P.** (2007). KIN-29 SIK regulates chemoreceptor gene expression via an MEF2 transcription factor and a class II HDAC. *EMBO J.* **26**, 358-370.
- Vega, R. B., Matsuda, K., Oh, J., Barbosa, A. C., Yang, X., Meadows, E., McAnally, J., Pomajzl, C., Shelton, J. M., Richardson, J. A. et al.** (2004). Histone deacetylase 4 controls chondrocyte hypertrophy during skeletogenesis. *Cell* **119**, 555-566.
- Wang, B., Moya, N., Niessen, S., Hoover, H., Mihaylova, M. M., Shaw, R. J., Yates, J. R., 3rd, Fischer, W. H., Thomas, J. B. and Montminy, M.** (2011). A hormone-dependent module regulating energy balance. *Cell* **145**, 596-606.
- Woods, A., James, C. G., Wang, G., Dupuis, H. and Beier, F.** (2009). Control of chondrocyte gene expression by actin dynamics: a novel role of cholesterol/Ror-alpha signalling in endochondral bone growth. *J. Cell. Mol. Med.* **13**, 3497-3516.
- Zhao, Q., Eberspaecher, H., Lefebvre, V. and De Crombrughe, B.** (1997). Parallel expression of Sox9 and Col2a1 in cells undergoing chondrogenesis. *Dev. Dyn.* **209**, 377-386.

**Table S1. Primers**

<b>Cloning</b>		
Target	Primer	Sequence
<i>Hdac4</i>	Forward	CGGAATTCCGATGAGCTCCCAAAGCCATCCAGATG
	Reverse	GCTCTAGAGCCTACAGTGGTGGTTCCTCCTCCATG
<i>Mef2c</i>	Forward	GAAGATCTTCATGGGGAGAAAAAAGATTTCAGATTACGAGG
	Reverse	GCTCTAGAGCTCATGTTGCCCATCCTTCAGAGAG
<b>Quantitative PCR</b>		
<i>Vegf</i>	Forward	GCACATAGAGAGAATGAGCTTCC
	Reverse	CTCCGCTCTGAACAAGGCT
<i>Vegfr</i>	Forward	TGGCTCTACGACCTTAGACTG
	Reverse	CAGGTTTGACTTGTCTGAGGTT
<i>Hif1a</i>	Forward	ACCTTCATCGGAAACTCCAAAG
	Reverse	CTGTTAGGCTGGGAAAAGTTAGG
<i>Hif2a</i>	Forward	CTGAGGAAGGAGAAATCCCGT
	Reverse	TGTGTCCGAAGGAAGCTGATG
<i>Ank</i>	Forward	CAGTCAAGGAGGATGCAGTAGA
	Reverse	CACTGTAGGCTATCAGGGTGT
<i>Enpp</i>	Forward	CTGGTTTTGTCTAGTATGTGTGCT
	Reverse	CTCACCGCACCTGAATTTGTT